

Enhanced down conversion of photons emitted by photoexcited $\text{Er}_x\text{Y}_{2-x}\text{Si}_2\text{O}_7$ films grown on silicon

Maria Miritello,^{1,2,*} Roberto Lo Savio,^{1,2} Paolo Cardile,^{1,2,3} and Francesco Priolo^{1,2,3}

¹*MATIS CNR-INFN, via S. Sofia 64, 95123 Catania, Italy*

²*Dipartimento di Fisica e Astronomia, Università di Catania, via S. Sofia 64, 95123 Catania, Italy*

³*Scuola Superiore di Catania, via S. Nullo 5/i, 95123 Catania, Italy*

(Received 20 November 2009; published 15 January 2010)

Photon cutting with efficiencies up to 400% is demonstrated in $\text{Er}_x\text{Y}_{2-x}\text{Si}_2\text{O}_7$ films grown on Si and its concentration dependence is analyzed. The cutting is the result of cross-energy-transfer processes occurring within a single rare earth (Er^{3+}) acting as both sensitizer and activator. Similarities with upconversion are revealed and possible applications in solar cells are discussed.

DOI: [10.1103/PhysRevB.81.041411](https://doi.org/10.1103/PhysRevB.81.041411)

PACS number(s): 78.55.-m, 71.20.Eh

The improvement of solar cell efficiencies represents an important technological challenge requiring the exploitation of new fundamental physical effects.¹ One of the main limitations in photovoltaics is represented by the fact that when a photon is absorbed into a semiconductor cell the generated electron-hole couple releases very rapidly the energy in excess of the band gap into heat. This is particularly dramatic for ultraviolet and green photons and it represents a fundamental limit to the maximum efficiency achievable. An ideal solution to this problem would be a capping material able to down convert each high-energy photon into several low-energy parts before the interaction with the actual solar cell occurs.

Rare-earth (RE) ion-doped materials have attracted for a long time the interest of the scientific community for the wide application in optical communications and lasers.² Most recently potential applications as down converters have also emerged. The simultaneous transfer of excitation energy from a sensitizer to an activator transforms a high-energy photon into two (or more) photons of lower energy, hence “cutting” the energy quantum.³ While most of the published works report two-photon quantum cutting using two different RE ions^{3–8} or by exploiting the energy transfer between the host, acting as a sensitizer, and one RE ion,^{9,10} a higher efficiency has been achieved through multiple exciton generation in semiconductor quantum dots.^{11–13} Here, through a careful tuning of the optical properties of $\text{Er}_x\text{Y}_{2-x}\text{Si}_2\text{O}_7$ films, we will demonstrate that by using a single RE (Er^{3+}) as both sensitizer and activator a quantum cutting with an efficiency up to 400% can be achieved.

$\text{Er}_x\text{Y}_{2-x}\text{Si}_2\text{O}_7$ is a material in which it is possible to increase gradually the Er content, in such a way that Er passes continuously from a regime where it is a dopant to a regime in which it is a constituent. This is made possible by the similar chemical properties of Y^{3+} and Er^{3+} and by their ionic radii (0.90 and 0.89 Å, respectively¹⁴) which allow the two ions to concur in the occupation of similar lattice sites. However, since Y^{3+} is optically inactive, in this way one can finely control the Er^{3+} pair interactions and maximize the desired effects.

Erbium-yttrium disilicate thin films, about 130 nm thick, have been grown in an ultrahigh vacuum magnetron sputtering system on (100) *c*-Si substrates heated at 400 °C by

radio frequency (rf) cosputtering from Er_2O_3 , Y_2O_3 , and SiO_2 targets. Further details on the apparatus and on the deposition procedure can be found elsewhere.^{15,16} Different compositions were synthesized by changing the rf powers applied to the targets and analyzed by Rutherford backscattering spectrometry. The Er content was measured between 2×10^{20} and 1.50×10^{22} cm⁻³ in erbium yttrium disilicate films, $\text{Er}_x\text{Y}_{2-x}\text{Si}_2\text{O}_7$, corresponding to *x* values between 0.03 and 2. Deposited films are amorphous and after rapid thermal annealing at 1200 °C for 30 s in O_2 ambient crystallize in a mixture of the γ and α phases typical of rare-earth disilicates, as already observed for $\text{Er}_2\text{Si}_2\text{O}_7$ thin films.¹⁵ The crystalline structure is independent of the Er content, as verified by x-ray diffraction. The refractive indices were evaluated by ellipsometric measurements performed with an He-Ne laser at 632.8 nm.

Room-temperature photoluminescence (PL) measurements were performed by pumping with the 2.54 eV line of an Ar^+ laser. The light was chopped through an acousto-optic modulator at a frequency of 11 Hz, analyzed by a single grating monochromator, and detected by a Hamamtsu infrared extended photomultiplier tube cooled at liquid-nitrogen temperature coupled with a lock-in amplifier having the modulation frequency as a reference.

All the samples show an intense PL emission peaked at 1.54 μm associated with the Er^{3+} de-excitation from the $^4I_{13/2}$ to the $^4I_{15/2}$ level. No other PL peaks are detected. The inset of Fig. 1 reports the PL spectra obtained for *x* values between 0.03 and 2 under a pump photon flux, ϕ , of 1×10^{19} cm⁻² s⁻¹. The shapes appear unchanged independently of *x*, demonstrating that in all cases the emitting ions are in the same environment, typical of Er^{3+} ions in the α phase of the RE disilicate, as already observed for $\alpha\text{-Er}_2\text{Si}_2\text{O}_7$.^{15,16} The observed peak PL intensity increases with increasing the Er content. However, passing from *x*=0.03 to *x*=2, corresponding to an increase in the Er content by about a factor of 70 the intensity is increased by only a factor of 10. This suggests that $\text{Er}^{3+}\text{-Er}^{3+}$ interactions depleting the first excited level $^4I_{13/2}$, such as upconversion phenomena, might influence the PL emission at the higher Er contents. In order to characterize these effects we have measured the PL intensity (I_{PL}) at 1.54 μm as a function of ϕ in the range $10^{18}\text{--}10^{22}$ cm⁻² s⁻¹. The data are shown in Fig. 1

for three samples having $x=0.03$, 0.65, and 2. The PL intensity increases linearly and then exhibits a sublinear increase associated with the upconversion phenomenon where two Er^{3+} ions both excited at the ${}^4I_{13/2}$ level interact, with one being de-excited to the ${}^4I_{15/2}$ ground state and the other being resonantly excited to the ${}^4I_{9/2}$ level,¹⁷ as schematically depicted on the left-hand corner. The final effect is a depletion of the first excited level. Of course this effect should be more severe at high Er contents and high pump powers. In fact we observe that by increasing the Er concentration the linear regime is limited to a narrower flux range, owing to the reduction in the Er^{3+} - Er^{3+} distance and therefore to the more efficient dipole-dipole interaction, thus determining an increase in the upconversion rate. Note that for all the samples under an excitation flux of $1 \times 10^{19} \text{ cm}^{-2} \text{ s}^{-1}$ used for the data reported in the inset of Fig. 1 the regime is always linear, suggesting that in this flux range upconversion phenomena are negligible. At low pump powers, however, a nonradiative concentration quenching process may occur. In this case the excitation is resonantly transferred from one excited Er^{3+} ion to a nearby Er^{3+} ion in the ground state and hence it travels along the sample. The excitation is eventually lost when a quenching center is encountered.¹⁷ The influence of concentration quenching has been evaluated by the decay time measurements for this low excitation condition. The curves have a simple exponential behavior in all the cases and the obtained lifetime values (τ) decrease monotonically from 5.6 to 0.27 ms by increasing the x value from 0.03 to 2, as a result of the gradual mean Er^{3+} - Er^{3+} distance reduction.

In the studied linear regime the PL intensity follows the relationship

$$I_{\text{PL}} = \eta \sigma \phi N_{\text{Er}} \frac{\tau}{\tau_{\text{RAD}}}, \quad (1)$$

with η being the detection efficiency, σ being the effective excitation cross section, N_{Er} being the total Er content, and τ_{RAD} being the radiative lifetime. Since the measurements have been performed under the same excitation conditions, by exciting Er^{3+} ions resonantly to the ${}^4F_{7/2}$ level, η and ϕ are the same for all the analyzed cases. Moreover, since the Er de-excitation can be described as an electrical dipole transition following the Fermi golden rule, the spontaneous emission probability, and therefore the inverse of the radiative lifetime τ_{RAD} , has a squared dependence on the medium refractive index.¹⁸ Ellipsometric measurements have shown that the refractive index is 1.77 ± 0.02 for all the samples; therefore, we conclude that τ_{RAD} is constant independent of x in $\text{Er}_x\text{Y}_{2-x}\text{Si}_2\text{O}_7$. If we report the experimentally determined ratio $I_{\text{PL}}/(N_{\text{Er}}\tau)$ normalized to the value obtained for the lowest x value, as a function of N_{Er} , we have indeed a plot of σ/σ_0 , i.e., of the effective cross section σ normalized to its low concentration value σ_0 , as shown in Fig. 2(a). In principle, the excitation cross section is expected to be similar for all samples since the excitation due to direct photon absorption involves the same atomic transition of Er^{3+} ions in a similar environment. In contrast, three different concentration regimes are visible: up to $x=0.40$ σ remains constant,

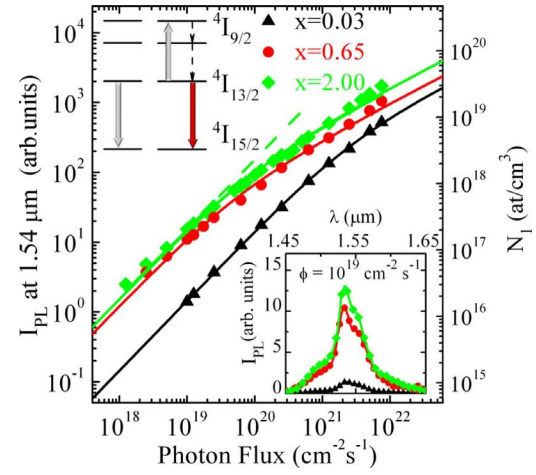


FIG. 1. (Color online) PL intensity at $1.54 \mu\text{m}$ as a function of pump photon flux ϕ of the samples with $x=0.03$, 0.65, and 2. The continuous curves are fits of the experimental data for the three samples, obtained by using relation (3), the dashed curve is the linear fit in the low excitation regime for the sample with $x=2$. The inset (on the right corner) reports the PL spectra of the three samples for $\phi=1 \times 10^{19} \text{ cm}^{-2} \text{ s}^{-1}$. In all the cases the excitation energy is 2.54 eV of an Ar^+ laser. A scheme of the upconversion phenomenon is depicted on the left-hand corner.

for $x \geq 0.65$ it increases by about a factor of 2, and for $x=2$ it reaches the maximum value of about 3.

A confirmation of these higher effective excitation cross sections at increasing Er contents is also given by fitting the I_{PL} trend at $1.54 \mu\text{m}$ as a function of ϕ in Fig. 1. In fact, if we describe the system by a two-level model only by neglecting the population of the levels lying at energies higher than ${}^4I_{13/2}$, as confirmed by their rapid de-excitations,¹⁹ the rate equation can be described by²⁰

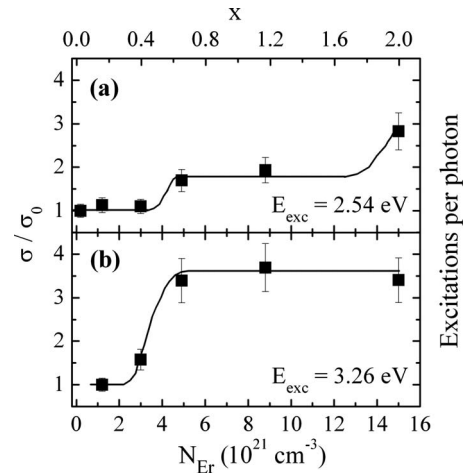


FIG. 2. σ/σ_0 , i.e., the effective cross section σ normalized to its low concentration value σ_0 , or number of excitations per photon as a function of Er concentration in $\text{Er}_x\text{Y}_{2-x}\text{Si}_2\text{O}_7$ films under (a) 2.54 eV and (b) 3.26 eV excitation. The lines are guide for the eyes.

$$\frac{dN_1(t)}{dt} = \sigma\phi(N_{\text{Er}} - N_1(t)) - \frac{N_1(t)}{\tau} - C_{\text{up}}[N_1(t)]^2, \quad (2)$$

where $N_1(t)$ is the Er^{3+} population in the first ${}^4I_{13/2}$ excited level at the time t and C_{up} is the upconversion coefficient. By considering the steady-state condition we obtain

$$N_1 = \frac{1}{2C_{\text{up}}\tau} \left[\sqrt{1 + \sigma\phi\tau(2 + 4C_{\text{up}}N_{\text{Er}}\tau + \sigma\phi\tau)} - (1 + \sigma\phi\tau) \right]. \quad (3)$$

The PL intensity reported in Fig. 1 can indeed be converted to the Er^{3+} population in the first excited level, N_1 (right-hand scale), by means of a proper calibration procedure using an Er-doped silica sample as a reference. In the calculation procedure it was assumed that all Er^{3+} in silica is optically active and the differences in τ_{rad} and in light extraction efficiencies among samples have been properly taken into account following a procedure already well established in the literature.²¹ The data in Fig. 1 can be fitted with Eq. (3) and it is possible to extract C_{up} values. By considering as the effective excitation cross section for $x=0.03$ the known value of the absorption cross section under 2.54 eV resonant excitation for Er-doped silicate glasses,²² $2.2 \times 10^{-21} \text{ cm}^2$, while for $x=0.65$ and 2, respectively, two and three times this value, as suggested by Fig. 2(a), the curves—reported in Fig. 1 as continuous lines—well fit the experimental data. Note that assuming a single effective cross section σ for all three samples it is instead impossible to obtain a reasonable fit. This is a further evidence of the dependence of σ on the Er content. Moreover, the fits give us also an estimation of C_{up} values of $(2.3 \pm 0.6) \times 10^{-17}$, $(6.4 \pm 0.9) \times 10^{-16}$, and $(1.1 \pm 0.1) \times 10^{-15} \text{ cm}^3/\text{s}$, respectively, for $x=0.03$, 0.65, and 2. The C_{up} value obtained for the low Er-doped disilicate is on the same order of magnitude of that reported for Er-doped silica,²³ while the increase in the C_{up} value with increasing Er contents can be ascribed to the smaller distances among Er^{3+} excited pairs.

The simultaneous increase in both C_{up} and σ for the high Er concentration regime strongly suggests that the two processes have a common root. In fact the increased effective excitation cross section observed for the high Er^{3+} concentration regime [Fig. 2(a)] can easily be explained as the result of cross-energy-transfer processes involving the highly excited Er^{3+} ions (${}^4F_{7/2}$) having absorbed an incoming photon and the Er^{3+} population in the ground state ${}^4I_{15/2}$ (N_0), with a final result of multiple excitations with a single incoming excitation photon. These processes can become competitive with the fast nonradiative relaxation processes of the involved levels when the Er^{3+} - Er^{3+} interactions are more efficient. They involve a resonant Er^{3+} - Er^{3+} energy transfer, as in the case of upconversion, and as a first approximation we can consider as an estimate an interaction coefficient similar to the experimentally determined C_{up} values. Therefore, the characteristic time of interaction between an excited Er^{3+} ion and a nearby one in the ground state can be estimated to be $\sim (N_{\text{Er}}C_{\text{up}})^{-1}$, since $N_{\text{Er}} \approx N_0$ under these low excitation conditions. This value varies from about 200 μs for $x=0.03$, to 0.3 μs for $x=0.65$, and to 0.06 μs for $x=2$. This means that

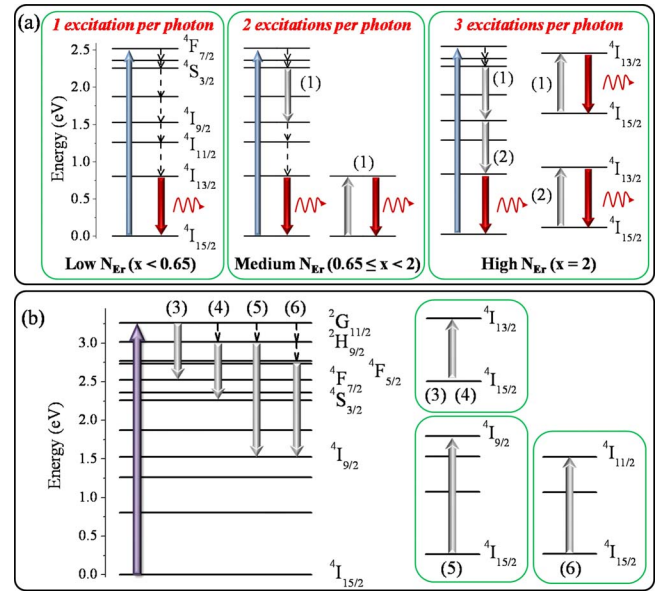


FIG. 3. (Color online) Schematic pictures of the cross-energy-transfer processes involving Er^{3+} ions under (a) 2.54 and (b) 3.26 eV excitations. Dashed lines indicate nonradiative phononic decays, light gray bold arrows indicate the transitions associated with the cross-energy transfers, the dark bold arrows indicate the radiative transition ${}^4I_{13/2} \rightarrow {}^4I_{15/2}$.

the Er^{3+} - Er^{3+} interaction strength strongly increases by increasing the Er^{3+} content. For this reason in the low Er-doping regime, under the 2.54 eV excitation, all the excited Er^{3+} ions to the ${}^4F_{7/2}$ level de-excite nonradiatively to the first excited level (${}^4I_{13/2}$) by subsequent nonradiative de-excitations [left panel in Fig. 3(a)]. One incoming photon is hence producing a single excitation. In contrast at higher Er concentrations the very rapid times of the Er^{3+} - Er^{3+} interaction make it more probable the occurrence of energy-transfer processes before multiphonon relaxation can take place. For instance, after the very rapid relaxation of ${}^4F_{7/2} \rightarrow {}^4S_{3/2}$ the ${}^4S_{3/2}$ level has a relaxation time of 5 μs . This means that for Er^{3+} contents higher than $x=0.65$ Er^{3+} - Er^{3+} interactions are faster and a resonant energy transfer (${}^4S_{3/2} \rightarrow {}^4I_{9/2}$, ${}^4I_{15/2} \rightarrow {}^4I_{13/2}$) can occur [process (1) in the center panel of Fig. 3(a)]. This is a real quantum cutting phenomenon since a single incoming photon is producing two excitations. The ion excited at the ${}^4I_{9/2}$ level can then decay nonradiatively to ${}^4I_{11/2}$ and ${}^4I_{13/2}$ with a characteristic time of 0.3 μs . If the Er^{3+} concentration is high enough a further Er^{3+} - Er^{3+} interaction [process (2) in the right panel of Fig. 3(a)] can be faster than multiphonon relaxation and leads to a further excitation. The initial green photon has hence produced three infrared photons. The enhanced effective excitation cross section in Fig. 2(a) is therefore a clear indication of quantum cutting with an efficiency up to 300% as a result of a competition between Er^{3+} - Er^{3+} interaction and multiphonon relaxation. The intimate meaning of the enhanced σ is an enhanced number of Er^{3+} excitations per photon, as clearly evidenced by the right-hand scale of Fig. 2. The important aspect we would like to stress is that quantum cutting is occurring in a system with a single RE species as both sensitizer and activator and the process appears to be

strongly related to upconversion, with the important difference that upconversion, involving interactions among excited levels, requires high excitation photon fluxes, while photon cutting, requiring the interaction with ground-state RE ions, occurs in the low pump power regime.

One question arises on the possibility of obtaining even higher quantum cutting efficiencies. In order to explore this possibility we have pumped the system at an excitation energy of 3.26 eV extracted from a Xe lamp and properly selected through a monochromator. The PL intensity at 1.54 μm was measured and the trend of σ/σ_0 as a function of N_{Er} has been evaluated [Fig. 2(b)]. In such conditions the Er^{3+} ions in the $\text{Er}_x\text{Y}_{2-x}\text{Si}_2\text{O}_7$ films are directly excited to the ${}^2G_{11/2}$ level, having an energy that corresponds to about four times the energy gap between the ground and the first excited states; as a consequence, a maximum increase by a factor of 4 of the effective excitation cross section for the ${}^4I_{13/2}$ level should be expected. Indeed the experimentally determined excitations per photon reach a maximum value very close to 4. However, this value is reached at 4.9×10^{21} Er/cm^3 ($x=0.65$), while under the 2.54 eV excitation the maximum value (about 3) was reached only in $\text{Er}_2\text{Si}_2\text{O}_7$ (1.50×10^{22} Er/cm^3 , $x=2$).

In order to explain such a different behavior it is necessary to take into account the further cross-energy-transfer processes that may occur under the 3.26 eV excitation. They are depicted in Fig. 3(b) as processes (3)–(6). In particular through processes (3) and (4) one Er^{3+} ion directly excited to the ${}^2G_{11/2}$ level, by absorbing one photon, decays to ${}^4F_{7/2}$ and to ${}^4S_{3/2}$, respectively; at the same time another ion in the ground state is resonantly promoted to ${}^4I_{13/2}$. In both cases the highly excited Er^{3+} ion may then follow the same de-excitation path already described in Fig. 3(a). Therefore, three or four Er^{3+} ions may be excited at the ${}^4I_{13/2}$ level for each absorbed photon. Moreover, process (5) brings two Er^{3+}

ions in the ${}^4I_{9/2}$ level. This may determine four, three, or two excitations, depending on whether it is followed or not by process (2). Up to three excitations may be obtained through process (6) followed by process (2).

The nonradiative decay times of the levels ${}^2G_{11/2}$, ${}^2H_{9/2}$, and ${}^4F_{5/2}$ are very fast, included between 0.2 and 0.4 μs , comparable to that of ${}^4I_{9/2}$. Therefore, in principle each of the four cross-energy-transfer processes (3)–(6) should become probable only for Er amounts well above 4.9×10^{21} at/cm^3 ($x=0.65$), as previously observed for process (2) involving ${}^4I_{9/2}$. Since under the 3.26 eV excitation the number of possible decay paths for each excited Er^{3+} ion is increased, the probability that at least one among them occurs also for lower Er amounts increases. This explains why an efficient quantum cutting occurs already at lower Er concentrations with respect to the case of the 2.54 eV excitation.

In conclusions, we have demonstrated that a proper tuning of the Er content in $\text{Er}_x\text{Y}_{2-x}\text{Si}_2\text{O}_7$ thin films enables cross-energy-transfer processes, typically deleterious for amplifying active materials, which become fundamental for the occurrence of quantum cutting of green and ultraviolet photons with an efficiency up to 400%. While it should be clear that not all photons but only those in resonance with the RE ion absorption spectrum can indeed be cut, the many multiplets present into the RE energy levels (Fig. 3) ensure that a non-negligible fraction of high-energy photons can indeed interact with the RE materials. In principle, these materials can hence have an impact in solar cells where photons of several energies can be properly cut in many low-energy parts increasing the number of generated electron-hole pairs.

The authors wish to thank G. Franzò, F. Iacona, A. Irrera, M. G. Grimaldi, and A. M. Piro for several contributions and discussions, and C. Percolla and S. Tatì for expert technical assistance.

*maria.miritello@ct.infn.it

- ¹P. Würfel, *Physics of Solar Cells: From Basic Principles to Advanced Concepts* (Wiley-VCH, Berlin, 2009).
- ²M. J. F. Digonnet, *Rare-Earth-Doped Fiber Lasers and Amplifiers* (M. Dekker Inc., New York, 2001).
- ³R. T. Wegh *et al.*, *Science* **283**, 663 (1999).
- ⁴P. Vergeer, T. J. H. Vlught, M. H. F. Kox, M. I. den Hertog, J. P. J. M. van der Eerden, and A. Meijerink, *Phys. Rev. B* **71**, 014119 (2005).
- ⁵B. S. Richards, *Sol. Energy Mater. Sol. Cells* **90**, 1189 (2006).
- ⁶T. J. Lee *et al.*, *Appl. Phys. Lett.* **89**, 131121 (2006).
- ⁷S. Ye *et al.*, *Opt. Express* **16**, 8989 (2008).
- ⁸D. Q. Chen *et al.*, *Opt. Lett.* **33**, 1884 (2008).
- ⁹J. L. Sommerdijk, A. Bril, and A. W. Jager, *J. Lumin.* **8**, 341 (1974).
- ¹⁰S. Kück, I. Sokólska, M. Henke, T. Scheffler, and E. Osiaç, *Phys. Rev. B* **71**, 165112 (2005).
- ¹¹R. D. Schaller *et al.*, *Nano Lett.* **6**, 424 (2006).

¹²R. D. Schaller *et al.*, *Nat. Phys.* **1**, 189 (2005).

¹³D. Timmerman *et al.*, *Nat. Photonics* **2**, 105 (2008).

¹⁴R. D. Shannon, *Acta Crystallogr., Sect. A: Cryst. Phys., Diffr., Theor. Gen. Crystallogr.* **32**, 751 (1976).

¹⁵R. Lo Savio *et al.*, *Appl. Phys. Lett.* **93**, 021919 (2008).

¹⁶M. Miritello *et al.*, *Adv. Mater.* **19**, 1582 (2007).

¹⁷A. Polman, *J. Appl. Phys.* **82**, 1 (1997).

¹⁸W. Beall Fowler and D. L. Dexter, *Phys. Rev.* **128**, 2154 (1962).

¹⁹C. Li, C. Wyon, and R. Moncorge, *IEEE J. Quantum Electron.* **28**, 1209 (1992).

²⁰G. N. van den Hoven *et al.*, *J. Appl. Phys.* **79**, 1258 (1996).

²¹M. Wojdak, M. Klik, M. Forcales, O. B. Gusev, T. Gregorkiewicz, D. Pacifici, G. Franzò, F. Priolo, and F. Iacona, *Phys. Rev. B* **69**, 233315 (2004).

²²W. J. Miniscalco, *J. Lightwave Technol.* **9**, 234 (1991).

²³M. Federighi and F. Di Pasquale, *IEEE Photonics Technol. Lett.* **7**, 303 (1995).